

Surface Roughness Prediction in the Hardened Steel Ball-End Milling by Using the Artificial Neural Networks and Taguchi Method

Andrzej Matras¹

¹ Chair of Production Engineering, Mechanical Faculty, Cracow University of Technology, Al. Jana Pawła II 37, 31-864 Kraków, Poland

E-mail: andrzej.matras@pk.edu.pl

ABSTRACT

The paper provides an analysis of the impact of the values of cutting tool inclination strategies and angles measured in the parallel and perpendicular to feed direction, radial depth of cut and feedrate on the surface roughness. The workpiece was made of the AISI H13 steel, hardness 50 HRC, and was machined using a ball-nosed end mill with CBN edges. The research methodology involved experiments conducted based on the Taguchi orthogonal array, optimization of parameters with the use of Taguchi method and process modelling using neural networks. Thanks to the use of neural networks, the analyses were performed for various levels of machining efficiency, obtained as a result of different radial depths of cut and feedrates. In order to obtain mathematical models well-describing strongly nonlinear impact of the cutting tool inclination strategies and angles, a separate neural network learned for each tool inclination strategy. The prediction of results was made using a set of neural networks. The analyses and experiments resulted in surfaces with very low Ra parameter of 0.16 mm and mathematical models with a good fit to the experimental data. Values of the cutting tool inclination angle that allow obtaining the surface of specific surface roughness were specified for various levels of machining performance.

Keywords: hard milling, CBN, ball-nosed end mill, Artificial Neural Networks, Taguchi, roughness, industry, modelling.

INTRODUCTION

Cubic boron nitride (CBN) is an exceptionally hard material, maintaining its properties at high temperatures. Its hardness is evaluated at 90-95% of the hardness of diamond. It also maintains a high chemical resistance in contact with iron [1]. As a result, CBN is widely used to produce the edges of cutting tools [2]. Milling cutters with CBN edges allow machining of materials in hardened state, replacing traditional, low-efficiency grinding or electrical discharge machining processes by milling or turning [3-4]. Such approach makes it possible to reduce the machining time and production costs, limits the machine park and workpiece handling. This solution is becoming increasingly popular and many researchers study the use of cutting tools with CBN edges in machining of materials in hardened state. Waszczuk

et al. [5] have analysed the impact of the machining method and strategy on the surface roughness of materials in hardened state. Wang et al. [6] have compared the machining efficiency during high-speed milling with the use of tools made of fine-grained binder-less and conventional CBN. They have analysed the cutting forces, friction coefficient on the rake face, tool temperature and wear. Saketi et al. [7] have analysed the wear of a high CBN-content cutting tool during the machining of materials with different hardnesses. They have observed tool wear due to tribo-chemical reactions, adhesive wear and mild abrasive wear, and indicated the tendency to micro-chipping along the cutting edge especially at higher cutting speeds. Jin et al. [8] have developed ball-nosed end milling cutters with CBN edges for machining of hardened steels. Focusing on the tool production costs and shape accuracy and the

resistance of the cutting edge to micro-chipping, they have developed solutions that allow improve the surface roughness in finishing machining or increase the machining efficiency in the roughing machining. Sato et al. [9] have measured the temperature during the finish milling using a cutter with CBN edges. They have obtained a lower temperature for the down milling. Okada et al. [10] have machined a 60 HRC steel using a tool with CBN edges, and have noticed a strong impact of the cutting speed on the tool temperature. At 600 m/min the temperature was 850 °C.

Many researchers analyse the machining process of curvilinear surfaces using an inclined ball-nosed milling cutter [11]. Benio et al. [12] have suggested a sequence of steps taken in order to select the optimum strategy for milling of curvilinear surfaces. They have analysed the impact of the tool path on the surface roughness measured in the workpiece areas inclined at different angles. Based on a ANNs and orthogonal arrays, Zhou et al. [13] and Bilek et al. [14] have developed a method for multicriterial optimization of the cutting tool inclination angle measured in a single plane. Yao et al. [15] and De Souza et al. [16] have studied the impact of the cutting tool direction and angle during machining of a curvilinear surface using a carbide ball-nosed milling cutter. They have indicated that the best effects are obtained when during the machining the tool is kept at a fixed angle measured in relation to the machined surface. Matras and Zębala [17] have used a two-stage optimization of the machining of a curvilinear surface using a ball-nosed milling cutter with CBN edges. The cutting tool inclination angle is specified in the first stage, and then – depending on the workpiece shape – the feedrate is optimized based on the FEM calculations in order to obtain the surface with a uniform roughness.

Various techniques are used for modelling the machining process. Among the experiment-based techniques, the most often used experiment design techniques include the Taguchi Method, Response Surface Methodology (RSM) and increasingly popular modelling based on artificial neural networks (ANNs) [18]. Using the ANNs, it is possible to develop well-fitted to the experimental data mathematical models used to predict surface roughness[19-20]. Thanks to the ANNs, Mongan et al. [21] have developed models describing complex, nonlinear relations between the milling process parameters and its efficiency

and obtained surface roughness. Bilek et al. [22] using a neural network developed mathematical models for predicting surface roughness. Gupta et al. [23] have applied the Taguchi method for a multicriterial evaluation of the impact of cutting parameters on the quality of surface machined by using tools with CBN edges. Vishnu et al. [24] have applied the Taguchi Method and the RSM to optimize the impact of the cutting speed, feedrate as well as axial and radial depth of cut on the surface roughness. They have machined the P20 steel for which they have determined the optimal parameters, mentioning however that as a result of using both methods the optimum solution is analogous. The Taguchi method has also been used by Masmaiti et al. [25] who have optimized the machining using an inclined ball-nosed milling cutter with cemented carbide edges.

The literature review indicates that the design of experiment techniques and modelling with the use of artificial neural networks are efficient and effective methods which can be used to analyse the impact of the cutting tool inclination angle on the roughness of machined curvilinear surface. At the same time, it was noticed that the number of papers on the modelling of machining of curvilinear surfaces using CBN ball-nosed mills inclined simultaneously in the parallel and perpendicular to the feed direction is insufficient.

The paper describes the developed optimization method, based on modelling by using the artificial neural networks to determine the simultaneous effects of feed rate, radial depth of cut and tool tilt angles. Using the artificial neural network modelling, based on the same number of experimental studies as in the Taguchi method, surface roughness prediction was made for different levels of machining process efficiency, which is not possible in the Taguchi method. The application of the proposed method can improve the efficiency and precision of machining processes with superhard tooling materials, which will positively affect to the technology of manufacturing molds and dies machined in the hardened state.

MATERIALS AND METHODS

The studies involved machining of the AISI H13 steel hardened to 50 HRC. The chemical composition of AISI H13 is presented in Table 1.

The machining was performed using a Mitsubishi ball-nosed end mill with CBN edges,

Table 1. Chemical composition of the AISI H13 steel (wt%)

C	Mn	Si	Cr	Mo	V
0.4	0.4	1.0	5.25	1.35	1.0

Table 2. Geometry of the milling tool

R (mm)	D_1 (mm)	a_p (mm)	L_3 (mm)	D_5 (mm)	B_2 (°)	L_1 (mm)	D_4 (mm)
1	2	1.5	5	1.9	7.3	52	4

Table 3. Recommended cutting data values

n (rev/min)	v_c (m/min)	a_p (mm)	a_e (mm)	f (mm/min)
27000	150	0.1	0.035	1900

designated CBN2XLBR0100N050S04. A cutting edge geometry with a rake angle $g_o = 0^\circ$ and helix angle $l_s = 0^\circ$ was used. The cutting edge radius of the tool arc was $r_n = 1$ mm with a tolerance of ± 5 μ m. The geometrical parameters of the tool are presented in Table 2.

Recommended by tool producer cutting data values for the selected tool and workpiece material are presented in Table 3.

The machining was carried out on a five axis machine tool DMG Ultrasonic 20 linear. The studies aimed at determination of a simultaneous impact of the tool inclination direction and inclination

angle in the plane parallel (d_1) and perpendicular (d_2) to the tool feed direction, and the impact of the radial depth of cut (a_e) and the feedrate (f) on the microgeometry of the surface described by means values of the roughness parameter Ra . The tests were performed at constant cutting speed ($v_c = 150$ m/min), tool rotational speed ($n = 27\ 000$ rev/min) and depth of cut ($a_p = 0.1$ mm). Down milling was used, and the coolant was not used. The variability ranges of cutting parameters and the values of constant parameters were selected based on the literature review and the tool manufacturer’s recommendations. The range of applied

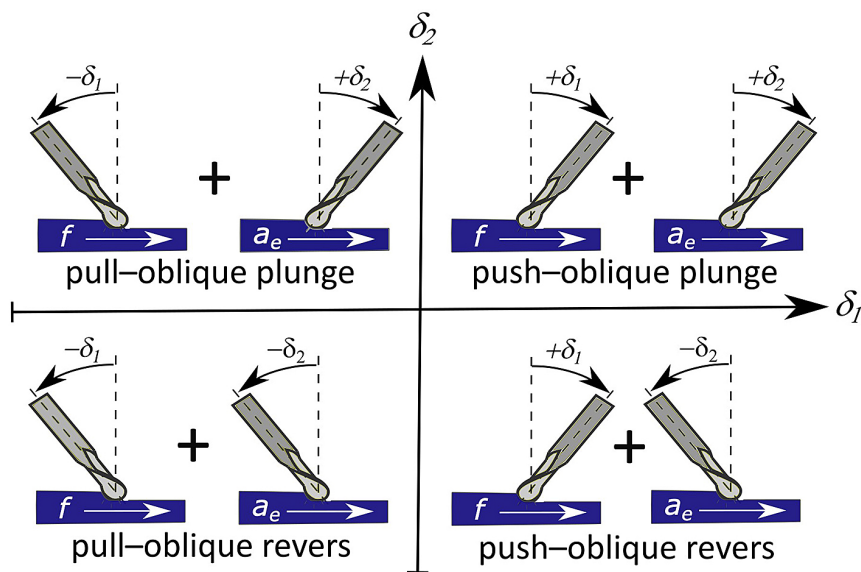


Fig. 1. The tool inclination directions for individual strategies directions (in view in a plane parallel and perpendicular to the feed)

cutting parameters corresponds to the HSC finish machining of curvilinear surfaces.

During the experimental tests, flat surfaces with dimensions of 5x5 mm were machined. The material used for the research was heat-treated and the variation in hardness is not more than ± 1 HRC. After fixing on the machine tool, the top surface of the specimens was milled, and then the tests planned were performed in the same fixture. As the studies are aimed at machining of curvilinear surfaces, this constituted a sort of simplification. However, it can be assumed that each curvilinear surface consists of fragments of straight surfaces of small dimensions measured in micrometres [26]. The experiments were conducted based on the L16 Taguchi orthogonal array. Depending on the tool inclination directions, four possible strategies were studied which corresponded to four analysed cases obtained by setting positive or negative values of tool inclination angles: push-oblique plunge (+ d_1 , + d_2), push-oblique reverse (+ d_1 , - d_2), pull-oblique reverse (- d_1 , - d_2) and pull-oblique plunge (- d_1 , + d_2).

The obtained tool inclination for individual strategies are presented in Figure 1.

Table 4 includes the applied levels of variable analysed parameters for each tool inclination strategy.

Sixty-four surfaces in total were made during the experiments. Each surface was measured three times and the Ra parameter was calculated, giving 192 data points. The measurements of the surface geometric microstructure were made using the profilograph Form TalySurf Intra 50. Measurements were made based on standards EUR 15178N, ISO 25178 and ISO 12781. The Taguchi method and artificial neural networks were used during the analyses.

The set values of the input factors along with the average value of surface roughness parameters Ra and standard deviations are shown in Table 5.

Depending on the tool inclination strategy, the corresponding signs from the first row in the table should be used for the tool inclination angles in the columns two and three.

Table 4. The applied levels of variable analysed parameters

No.	Case	a_e (mm)	f (mm/min)	d_1 (°)	d_2 (°)
1.	Push-oblique plunge	0.025; 0.05; 0.075; 0.1	720; 960; 1440; 1920	0; 6; 12; 18	0; 6; 12; 18
2.	Push-oblique revers	0.025; 0.05; 0.075; 0.1	720; 960; 1440; 1920	0; 6; 12; 18	-18; -12; -6; 0
3.	Pull-oblique revers	0.025; 0.05; 0.075; 0.1	720; 960; 1440; 1920	-18; -12; -6; 0	-18; -12; -6; 0
4.	Pull-oblique plunge	0.025; 0.05; 0.075; 0.1	720; 960; 1440; 1920	-18; -12; -6; 0	0; 6; 12; 18

Table 5. Average values and standard deviations for the parameter Ra

Parameters				Push-oblique plunge (+ d_1 , + d_2)		Push-oblique revers (+ d_1 , - d_2)		Pull-oblique revers (- d_1 , - d_2)		Pull-oblique plunge (- d_1 , + d_2)	
a_e (mm)	d_1 (°)	d_2 (°)	f (mm/min)	Ra (mm)	Std. Dev.						
0.025	0	18	960	0.20	0.077	0.23	0.045	0.29	0.074	0.17	0.016
0.025	6	12	720	0.17	0.003	0.18	0.005	0.16	0.004	0.20	0.007
0.025	12	6	1920	0.21	0.024	0.33	0.052	0.19	0.030	0.23	0.010
0.025	18	0	1440	0.28	0.011	0.26	0.021	0.15	0.010	0.20	0.007
0.050	0	12	1920	0.42	0.039	0.43	0.035	0.43	0.024	0.35	0.041
0.050	6	18	1440	0.30	0.051	0.19	0.010	0.22	0.019	0.20	0.010
0.050	12	0	960	0.27	0.047	0.27	0.004	0.31	0.077	0.16	0.018
0.050	18	6	720	0.19	0.005	0.24	0.020	0.18	0.010	0.22	0.049
0.075	0	6	1440	1.07	0.018	0.95	0.025	0.80	0.040	0.86	0.016
0.075	6	0	1920	0.68	0.030	0.66	0.053	0.68	0.037	0.58	0.048
0.075	12	18	720	0.18	0.012	0.28	0.027	0.24	0.012	0.24	0.004
0.075	18	12	960	0.21	0.014	0.30	0.015	0.22	0.009	0.31	0.046
0.100	6	6	960	1.03	0.047	0.50	0.017	0.48	0.035	0.41	0.009
0.100	12	12	1440	0.30	0.018	0.38	0.011	0.33	0.020	0.33	0.006
0.100	18	18	1920	0.40	0.017	0.41	0.026	0.34	0.023	0.51	0.013
0.100	0	0	720	0.38	0.073	0.38	0.073	0.38	0.073	0.38	0.073

RESULTS AND DISCUSION

ANOVA

The ANOVA was performed in order to determine the statistical significance of the analysed process parameters. The analysis was performed for the level of significance $\alpha = 0.05$. The analysis results for the Ra parameters are presented in Table 6.

The sensitivity of neural networks was also analysed. The sensitivity values greater than one indicate the statistical significance of the analysed input parameter. The analysis results are presented in Table 7.

The analysis of these tables 6-7 indicates that both ANOVA and the sensitivity analysis confirm that all analysed process parameters are statistically significant.

Optimization with the Taguchi method

The optimization with the Taguchi method was performed based on the “Smaller is better”. Such method is applied in order to minimize the value of the dependent variable. The ideal value of this variable is 0, and the measured value of the dependent variable must be equal to or greater

Table 6. ANOVA for the Ra parameters

Source	Push-oblique plunge					Push-oblique revers					Pull-oblique revers					Pull-oblique plunge				
	SS	df	MS	F	p	SS	df	MS	F	p	SS	df	MS	F	p	SS	df	MS	F	p
a_e	0.75	1	0.75	17.2	0.000	0.34	1	0.34	19.2	0.000	0.34	1	0.34	29.0	0.000	0.51	1	0.51	38.0	0.000
d_1	0.59	1	0.59	13.3	0.001	0.23	1	0.23	13.4	0.001	0.46	1	0.46	39.4	0.000	0.18	1	0.18	13.6	0.001
d_2	0.28	1	0.28	6.4	0.015	0.16	1	0.16	9.1	0.004	0.11	1	0.11	9.8	0.003	0.10	1	0.10	7.1	0.011
f	0.23	1	0.23	5.2	0.028	0.29	1	0.29	16.4	0.000	0.18	1	0.18	15.1	0.000	0.16	1	0.16	11.9	0.001
Error	1.89	43	0.04			0.75	43	0.02			0.50	43	0.01			0.58	43	0.01		
Total	3.74	47				1.77	47				1.59	47				1.54	47			

Table 7. Sensitivity analysis for the Ra parameter

Case	a_e (mm)	d_1 (°)	d_2 (°)	f (mm/min)
Push-oblique plunge	21.18	17.29	15.27	9.95
Push-oblique revers	66.93	39.97	37.30	29.49
Pull-oblique revers	12.65	11.12	5.64	2.77
Pull-oblique plunge	11.85	8.92	8.76	3.07

Table 8. The values of S/N ratios

a_e (mm)	d_1 (°)	d_2 (°)	f (mm/min)	S/N for push-oblique plunge ($+d_1, +d_2$)	S/N for push-oblique revers ($+d_1, -d_2$)	S/N for pull-oblique revers ($-d_1, -d_2$)	S/N for pull-oblique plunge ($-d_1, +d_2$)
0.025	0	18	960	14.159	12.930	10.810	14.438
0.025	6	12	720	15.437	15.028	15.687	14.121
0.025	12	6	1920	13.645	9.657	14.352	12.600
0.025	18	0	1440	11.066	11.670	16.752	14.100
0.050	0	12	1920	7.555	7.432	7.304	9.174
0.050	6	18	1440	10.649	14.447	13.369	13.918
0.050	12	0	960	11.614	11.427	10.500	12.332
0.050	18	6	720	14.224	12.374	14.764	13.214
0.075	0	6	1440	0.575	0.493	1.893	1.330
0.075	6	0	1920	3.395	3.626	3.387	4.704
0.075	12	18	720	14.960	11.191	12.412	12.293
0.075	18	12	960	13.580	10.488	13.098	9.865
0.100	6	6	960	0.240	6.057	6.416	7.686
0.100	12	12	1440	10.343	8.497	9.609	9.588
0.100	18	18	1920	7.936	7.696	9.284	5.931
0.100	0	0	720	10.359	8.972	8.533	6.539

than 0. For the analysis, the data were converted to the form expressed by equation (1).

$$\frac{S}{N} = -10 \cdot \log_{10} \left(\frac{\sum_{i=1}^n y^2}{n} \right) \quad (1)$$

where: n – number of cases;
 y – observed value of dependent variable.

The Table 8 includes the values of S/N ratios for the analysed strategies and the tool inclination angles, feedrate and radial depth of cut. Analogously to Table 5, suitable signs should be used for the tool inclination strategies.

The analysis based on the Taguchi method is conducted by analysing the plots representing the averaged impact of the studied parameters on the values of S/N ratios. The plots are presented in Figures 2a-d.

The analysis of these plots allows the determination of how to change the analysed parameters in order to minimize the Ra . For each of the studied tool inclination strategies there is one solution that ensures the least surface roughness.

In all analysed cases, this solution is obtained with the application of the lowest feedrate and the least radial depth of cut. The Taguchi method has a drawback in this aspect. The optimum solution is related to the least tested performance of the machining process. The optimum cutting tool inclination angles differ depending on the applied tool inclination strategy. For the push-oblique reverse and pull-oblique reverse strategies, they are $d_1 = 18^\circ$ and $d_2 = -18^\circ$, and $d_1 = -18^\circ$ and $d_2 = -18^\circ$, respectively; and for the push-oblique plunge and pull-oblique plunge strategies, they are $d_1 = 12^\circ$ and $d_2 = 18^\circ$, and $d_1 = -12^\circ$ and $d_2 = 18^\circ$.

Modelling with the use of neural networks

The multilayer perceptron (MLP) neural networks were used, because they are recommended for describing a nonlinear impact of input variables on the dependent variables (24). Such impact is observed for the studied process. The MLP neural network is learning in the supervised mode based on the previously created

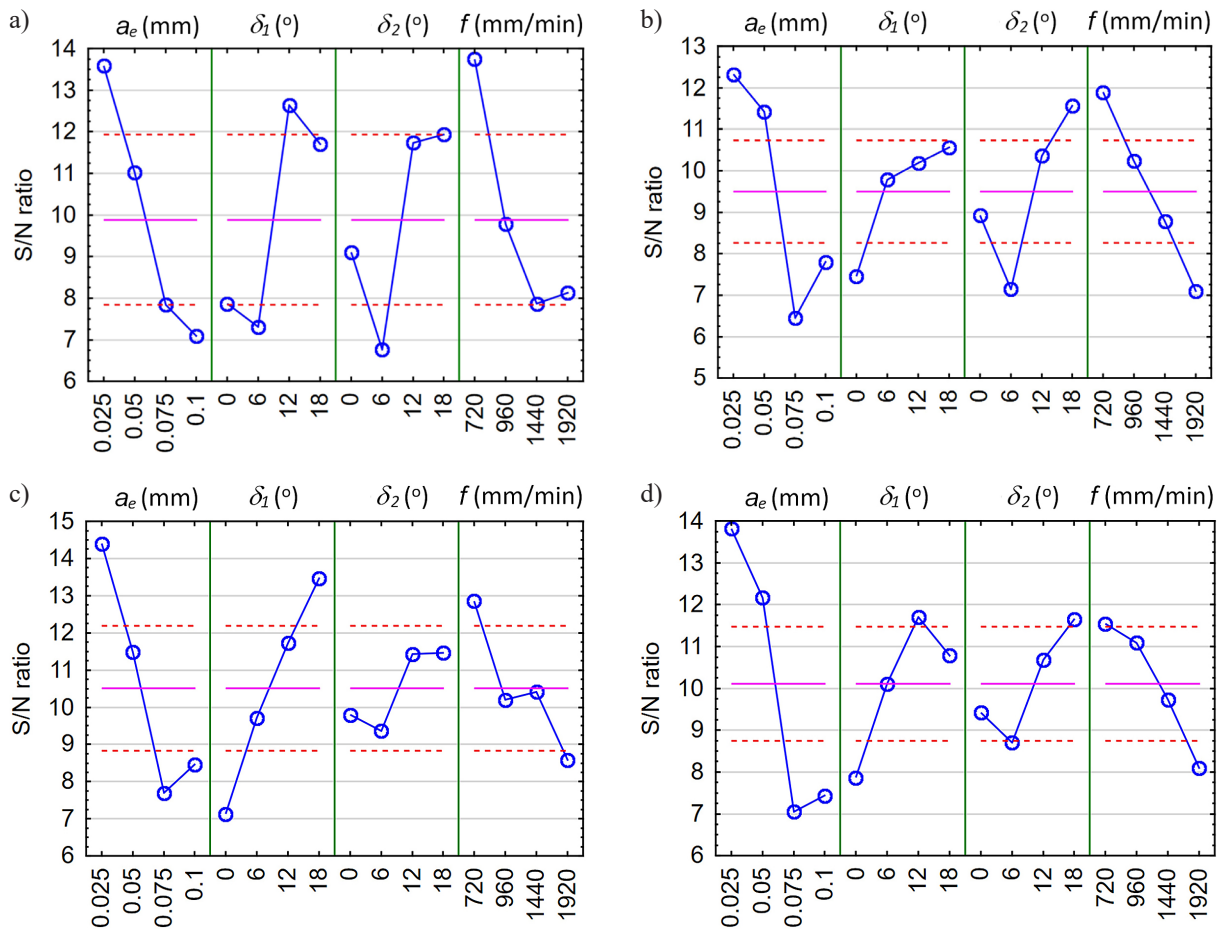


Fig. 2. The S/N ratios for a) push-oblique plunge tool inclination strategy, b) push-oblique reverse tool inclination strategy, c) pull-oblique reverse tool inclination strategy, d) pull-oblique plunge tool inclination strategy

set of observations. Four different networks were used, and each of them are learned based on the data from a different tool inclination strategy. The surface roughness values Ra were determined based on calculations performed with the use of a set of four neural networks. The networks architecture consisted of one hidden layer containing two neurons. As four input parameters and one output parameter were analysed, the input layer contained four neurons, and the output layer contained one. Such simple architecture prevents the network overfitting to the analysed data [27-29]. In order to choose four neural networks, a number of networks were generated and activated by means of various activation functions in the hidden and output layers. The following functions were used: linear (2), sigmoidal (3), exponential (4) and hyperbolic tangent (5). The argument in these functions is an aggregated signal connected with weights.

$$f(v) = v \tag{2}$$

$$f(v) = \frac{1}{1 + e^{-v}} \tag{3}$$

$$f(v) = e^{-v} \tag{4}$$

$$f(v) = \frac{e^v - e^{-v}}{e^v + e^{-v}} \tag{5}$$

where: v – aggregated signal connected with weights.

During the neural networks learning process, 70% of the data were learning data, 15% were the test data and 15% were the validation data. The networks learned with the use of the Broyden-Fletcher-Goldfarb-Shanno optimization algorithm. The error functions were determined as sums of squares (6).

$$E = \sum_{i=1}^n (y_i - t_i)^2 \tag{6}$$

where: y_i – observed value of dependent variable;
 t_i – predicted value of dependent variable.

When the learning process was completed for all neural networks, based on the best fit of validation data one network was selected for each four cutting tool inclination strategy. The Pearson correlation coefficients and the types of activation functions used in the hidden and output layers for selected four neural networks are presented in Table 9.

Table 10 includes the calculated values of Ra and values of remainders determined based on the average values from Ra measurements. Analogously to Table 5, suitable signs should be use for the tool inclination strategies.

The analysis of these tables indicates that the fit between the results calculated using the neural networks and the measurement data was good.

Successive figures include plots depicting the impact of the tool inclination strategies and the inclination angles on the surface roughness parameter Ra . The plots were made for different radial depths of cut (a_e), feedrates (f) and machining efficiency (Q_f) (7).

$$Q_f = a_e \cdot f \tag{7}$$

The calculated Ra values are presented with the use of a colour scale. Black lines are the borders of the areas determined based on the surface

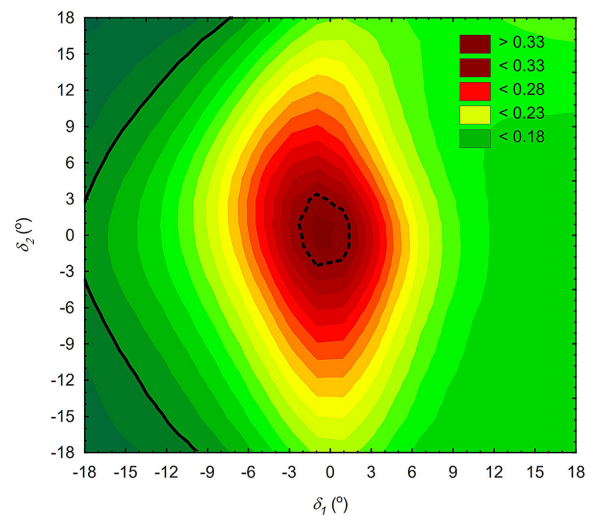


Figure 3. The impact of tool inclination strategies and angles for the Ra parameter: $f = 720$ mm/min, $a_e = 0.025$ mm, $Q_f = 18$ mm²/min

Table 9. The Pearson correlation coefficients and the types of activation functions

Case	Learning	Test	Validation	Total	Hidden	Output
Push-oblique plunge	0.98	0.97	0.97	0.98	hyperbolic tangent	logistic
Push-oblique revers	0.99	0.98	0.98	0.98	logistic	exponential
Pull-oblique revers	0.98	0.99	0.93	0.97	logistic	exponential
Pull-oblique plunge	0.97	0.94	0.98	0.97	hyperbolic tangent	logistic

Table 10. The calculated values of surface roughness Ra and values of remainders

Parameters				Push-oblique plunge (+ d_1 , + d_2)		Push-oblique revers (+ d_1 , - d_2)		Pull-oblique revers (- d_1 , - d_2)		Pull-oblique plunge (- d_1 , + d_2)	
a_e (mm)	d_1 (°)	d_2 (°)	f (mm/min)	Ra (mm)	Rem.						
0.025	0	18	960	0.21	-0.01	0.26	-0.03	0.22	0.07	0.19	-0.02
0.025	6	12	720	0.19	-0.02	0.18	0.00	0.18	-0.02	0.19	0.01
0.025	12	6	1920	0.27	-0.06	0.30	0.03	0.22	-0.03	0.18	0.05
0.025	18	0	1440	0.20	0.08	0.27	-0.01	0.18	-0.03	0.14	0.06
0.050	0	12	1920	0.40	0.02	0.43	0.00	0.44	-0.01	0.38	-0.03
0.050	6	18	1440	0.27	0.03	0.19	0.00	0.24	-0.02	0.20	0.00
0.050	12	0	960	0.28	-0.01	0.25	0.02	0.24	0.07	0.28	-0.12
0.050	18	6	720	0.19	0.00	0.24	0.00	0.19	-0.01	0.23	-0.01
0.075	0	6	1440	0.92	0.15	0.84	0.11	0.90	-0.10	0.99	-0.13
0.075	6	0	1920	0.66	0.02	0.66	0.00	0.62	0.06	0.66	-0.08
0.075	12	18	720	0.22	-0.04	0.28	0.00	0.20	0.04	0.31	-0.07
0.075	18	12	960	0.23	-0.02	0.30	0.00	0.21	0.01	0.28	0.03
0.100	6	6	960	1.01	0.02	0.50	0.00	0.48	0.00	0.36	0.05
0.100	12	12	1440	0.31	-0.01	0.37	0.01	0.34	-0.01	0.36	-0.03
0.100	18	18	1920	0.41	-0.01	0.40	0.01	0.32	0.02	0.50	0.01
0.100	0	0	720	0.38	0.00	0.32	0.06	0.39	-0.01	0.36	0.02

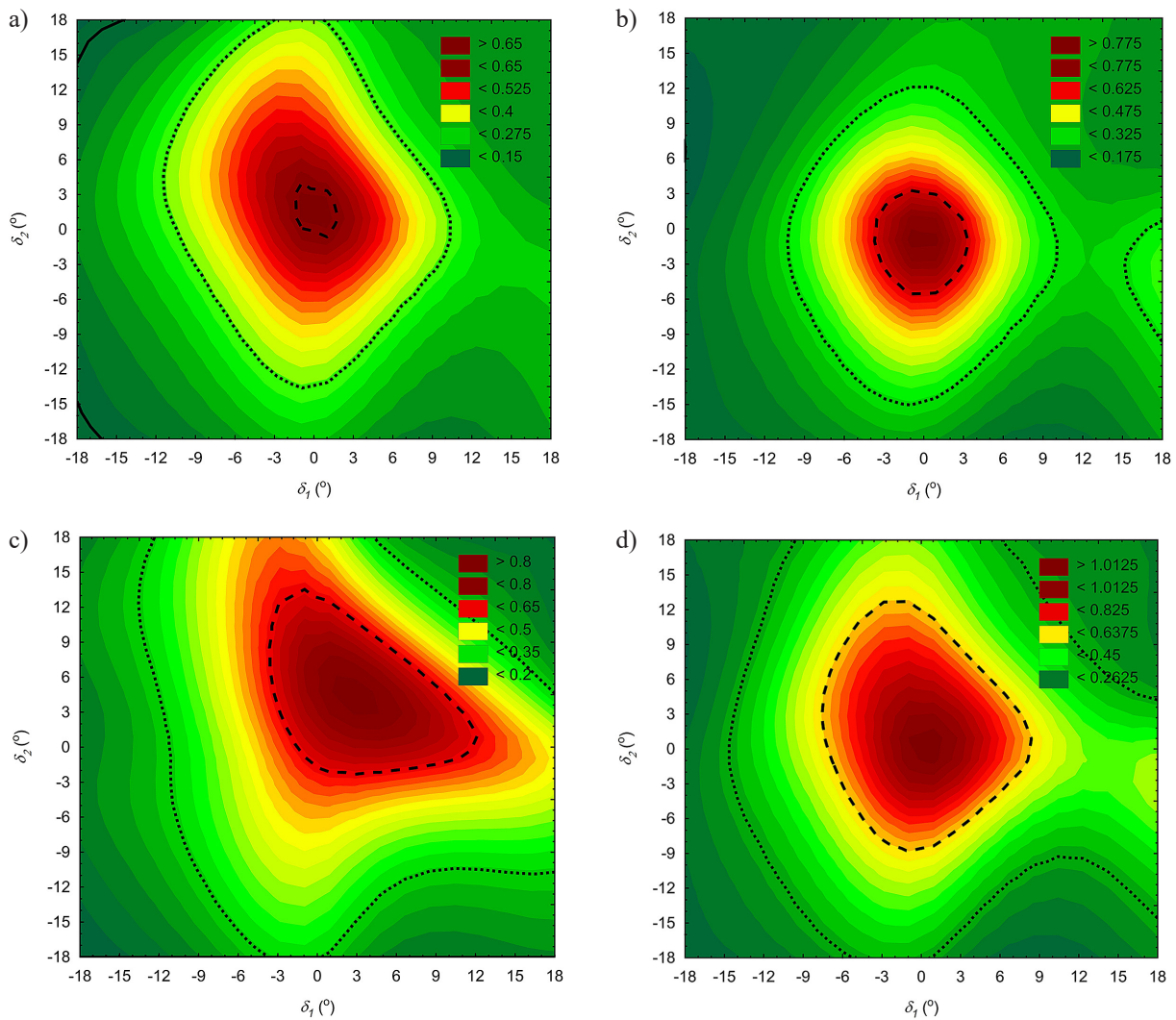


Fig. 4. The impact of tool inclination strategies and angles for the Ra parameter: a) $f=960$ mm/min, $a_e = 0.05$ mm, $Q_f = 48$ mm²/min, b) $f = 1440$ mm/min, $a_e = 0.05$ mm, $Q_f = 72$ mm²/min, c) $f = 960$ mm/min, $a_e = 0.075$ mm, $Q_f = 72$ mm²/min, d) $f = 1440$ mm/min, $a_e = 0.075$ mm, $Q_f = 108$ mm²/min

roughness classes according to the PN-EN ISO 1302:2004 standard. The $Ra = 0.16$ mm border was marked with a solid line, $Ra = 0.32$ mm with a dotted line, $Ra = 0.64$ mm with a broken line, $Ra = 1.25$ mm with a “long dash – short dash” line.

Figure 3 shows the impact of tool inclination strategies and angles for the least applied feedrates and radial depths of cut. These parameters allow achieving the efficiency equal to only $Q_f = 18$ mm²/min. For this machining efficiency, the expected surface roughness $Ra < 0,16$ mm can be achieved for angle $d_1 < -12^\circ$ and angle $d_2 > 15^\circ$ or $d_2 < -15^\circ$. Angle d_2 can be decreased with simultaneous decrease of angle d_1 . Surface roughness of 0.16–0.32 mm is obtained over a wide range of tool inclination directions and angles. Machining with small tool inclination angles ($-3^\circ < d_1 < 3^\circ$ and $-3^\circ < d_2 < 3^\circ$) gives surface roughness of $Ra > 0.32$ mm.

The impact of tool inclination strategies and angles observed for the medium analysed values of a_e and f are shown in figures 4a-d. Such a_e and f parameters give the machining efficiency Q_f in the 48–108 mm²/min range. When machining at $f = 920$ mm/min, $a_e = 0.05$ mm and tool inclination angles $d_1 = 18^\circ$ and $d_2 = 18^\circ$ or $d_2 = -18^\circ$ allowing $Q_f = 48$ mm²/min to be obtained, it is still possible to achieve $Ra < 0.16$ mm (Fig. 4a). This area is however small, and consequently it may be unique. Similarly to the situation above, a simultaneous increase of the tool inclination in both directions leads to reduced Ra values. For the surface machined at $f = 1440$ mm/min and $a_e = 0,075$ mm allowing $Q_f = 108$ mm²/min (Fig. 4d) to be obtained, the range of possible strategies

and tool inclination angles that give $Ra < 0.32$ mm is wide. The plots also indicate that inclining the tool in both directions is a better solution. Application of the pull-oblique reverse strategy gives the largest $Ra < 0.32$ mm area. The greater the f and a_e , the smaller the $Ra < 0.32$ mm area.

At the highest feedrates $f = 1920$ mm/min and greatest radial depths of cut $a_e = 0.1$ mm that allow obtaining the performance of $Q_f = 192$ mm²/min, it is still possible to achieve $Ra < 0.32$ mm (Fig. 5). In order to do this, it is recommended to use the tool inclination angles of $d_1 = 9^\circ$ and $d_2 = -18^\circ$ or $d_1 = -18^\circ$ and $d_2 = 6^\circ$. Application of each tested tool inclination strategy and both tool inclination angles from -9° to 9° allows achieving the surface roughness in the $0.64 < Ra < 1.25$ mm range. With the increase of feed rate and radial depth of cut, the positive effect of inclining the tool in both directions simultaneously is more visible. Figure 5 shows two areas of higher roughness. The first is for the case of machining with a non-inclined tool, while the second is for the case of inclining the tool only in the feed direction, where a worsening of surface roughness is observed for values of $d_1 > 15^\circ$. Roughness worsening is also observed when the tool is inclined only in the perpendicular direction to the feed. A non-inclined cutting tool gives the surface roughness of $Ra > 1.25$ mm.

CONCLUSIONS

The paper provides an analysis of the impact of the values of the cutting tool inclination strategies and angles measured in the parallel and perpendicular direction to the feed, radial depth of cut and feedrate on the surface roughness parameter Ra . The workpiece was made of the AISI H13 steel, hardness 50 HRC, and was machined using a 2 mm diameter ball-nosed end mill with CBN edges. The Taguchi method was applied in the first stage of the analysis. This allowed the determination of the tool inclination strategies and angles, and the feedrate and the depth of cut that would minimize the surface roughness parameter Ra . Due to a strongly nonlinear impact of the analysed cutting parameters, the analyses with the use of the Taguchi method were performed separately for each tool inclination strategy. In the second stage, the machining process was modelled with the use of neural networks. The analyses were performed

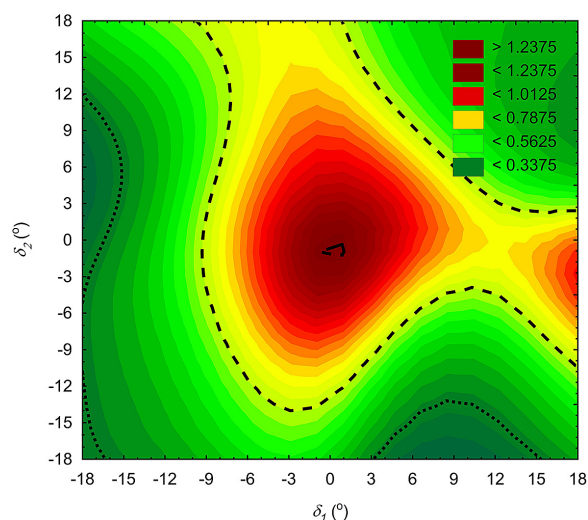


Fig. 5. The impact of tool inclination strategies and angles for the Ra parameter: $f = 1920$ mm/min, $a_e = 0.1$ mm, $Q_f = 192$ mm²/min

simultaneously for all tool inclination strategies and various feedrates and radial depths of cut.

The main conclusions about the investigated free surfaces milling are as followed:

1. As a result of the experimental research, surfaces with low surface roughness were obtained, the lowest observed value of the Ra parameter was 0.15 mm.
2. During machining with ball end mills, inclining the tool in the parallel and perpendicular direction to the feed results in a surface with a lower roughness than when the tool is inclined in only one direction. Machining with a non-inclined tool results in a worsening of surface roughness.
3. Taguchi Method is an unsatisfactory in case of simultaneous minimalization of surface roughness and optimization of tool inclination angles, feedrate and the depth of cut, because – due to the impact of the feed rate a result of the experimental research, surfaces with low surface roughness were obtained.
4. The radial depth of cut on the surface roughness the obtained optimum solution is related to low- efficiency machining.
5. The application of the modelling technique with the use of the artificial neural networks due to the possibility of simultaneous optimization of cutting tool inclination angles, feed speed, radial depth of cut and process efficiency will fill the demonstrated research gap.
6. Modelling with artificial neural networks resulted in mathematical models with a high fit to experimental data. All developed mathematical models were characterized by Pearson correlation coefficients values above 0.93.

The proposed research methodology in this paper can be successfully used in industrial applications. During its application, a relatively small experimental test is needed, and the measurement technology required for its application is available in the industrial sector. By using the proposed method, it is possible to minimize the basic problems identified in the mold and die machining. Development of the technological process considering application of the proposed method results in improvement of surface quality and machining efficiency.

REFERENCES

1. Devries R.C. Cubic Boron Nitride: Handbook of Properties. GE, 1972.
2. Du Y., Liang Z., Ma Y., et al. Development of PCBN

micro ball-end mill with multi-edge and spherical flank face. *J Manuf Process* 2022; 84: 424–434.

3. Vila C., Siller H.R., Rodriguez C.A., et al. Economical and technological study of surface grinding versus face milling in hardened AISI D3 steel machining operations. *Int J Prod Econ* 2012; 138: 273–283.
4. Soshi M., Fonda P., Kashihara M., et al. A study on cubic boron nitride (CBN) milling of hardened cast iron for productive and quality manufacturing of machine tool structural components. *Int J Adv Manuf Technol* 2013; 65: 1485–1491.
5. Waszczuk K., Karolczak P., Wisniewska M., et al. Influence of the path type on selected technological effects in the trochoidal milling. *Adv Sci Technol Res J* 2017; 11: 147–153.
6. Wang D., Yin L., Hänel A., et al. Cutting performance of binderless nano-polycrystalline cBN and PcBN milling tools for high-speed milling of hardened steel. *Ceram Int* 2023; 49: 34757–34773.
7. Saketi S., Sveen S., Gunnarsson S., et al. Wear of a high cBN content PCBN cutting tool during hard milling of powder metallurgy cold work tool steels. *Wear* 2015; 332–333: 752–761.
8. Jin M., Goto I., Watanabe T., et al. Development of cBN ball-nosed end mill with newly designed cutting edge. *J Mater Process Technol* 2007; 192–193: 48–54.
9. Sato M., Ueda T., Tanaka H. An experimental technique for the measurement of temperature on CBN tool face in end milling. *Int J Mach Tools Manuf* 2007; 47: 2071–2076.
10. Okada M., Hosokawa A., Tanaka R., et al. Cutting performance of PVD-coated carbide and CBN tools in hardmilling. *Int J Mach Tools Manuf* 2011; 51: 127–132.
11. Bilek O., Samek D., Suba O. Investigation of surface roughness while ball milling process. *Key Eng Mater* 2014; 581: 335–340.
12. Beňo J., Maňková I., Ižol P., et al. An approach to the evaluation of multivariate data during ball end milling free-form surface fragments. *Measurement* 2016; 84: 7–20.
13. Zhou J., Ren J., Yao C. Multi-objective optimization of multi-axis ball-end milling Inconel 718 via grey relational analysis coupled with RBF neural network and PSO algorithm. *Measurement* 2017; 102: 271–285.
14. Bilek O., Milde R., Strnad J., et al. Prediction and modeling of roughness in ball end milling with tool-surface inclination. *IOP Conf Ser Mater Sci Eng* 2020; 726: 012003.
15. Yao C., Tan L., Yang P., et al. Effects of tool orientation and surface curvature on surface integrity in ball end milling of TC17. *Int J Adv Manuf Technol* 2018; 94: 1699–1710.

16. de Souza A.F., Berkenbrock .E, Diniz A.E., et al. Influences of the tool path strategy on the machining force when milling free form geometries with a ball-end cutting tool. *J Braz Soc Mech Sci Eng* 2015; 37: 675–687.
17. Matras A., Zębala W. Optimization of Cutting Data and Tool Inclination Angles During Hard Milling with CBN Tools, Based on Force Predictions and Surface Roughness Measurements. *Materials* 2020; 13: 1109.
18. Srinivas M.S., Sangeeth P., Venkaiah N., et al. State of the art on tool wear characterization in micro-milling. *Mater Today Proc* 2023.
19. Kulisz M., Zagórski I., Józwiak J. 2D Geometric Surface Structure ANN Modeling after Milling of the AZ91D Magnesium Alloy. *Adv Sci Technol Res J* 2022; 16: 131–140.
20. Rifai A.P., Aoyama H., Tho N.H., et al. Evaluation of turned and milled surfaces roughness using convolutional neural network. *Measurement* 2020; 161: 107860.
21. Mongan P.G., Hinchy E.P., O’Dowd N.P., et al. An ensemble neural network for optimising a CNC milling process. *J Manuf Syst* 2023; 71: 377–389.
22. Bilek O., Samek D.. Neural networks in modeling of CNC milling of moderate slope surfaces. *Adv Intell Syst Comput* 2014; 285: 75–83.
23. Gupta A., Shah R., Dave H., et al. Multi-objective optimization of surface parameters such as concavity, straightness and roughness in milling process. *Mater Today Proc* 2018; 5: 5296–5302.
24. Vishnu Vardhan M., Sankaraiah G., Yohan M., et al. Optimization of Parameters in CNC milling of P20 steel using Response Surface methodology and Taguchi Method. *Mater Today Proc* 2017; 4: 9163–9169.
25. Masmiaati N., Sarhan A.A.D. Optimizing cutting parameters in inclined end milling for minimum surface residual stress – Taguchi approach. *Measurement* 2015; 60: 267–275.
26. Bouzakis K.-D., Aichouh P., Efstathiou K. Determination of the chip geometry, cutting force and roughness in free form surfaces finishing milling, with ball end tools. *Int J Mach Tools Manuf* 2003; 43: 499–514.
27. Haykin S. *Neural networks: a comprehensive foundation*. Prentice Hall PTR, 1998..
28. Machno M., Matras A., Szkoda M. Modelling and Analysis of the Effect of EDM-Drilling Parameters on the Machining Performance of Inconel 718 Using the RSM and ANNs Methods. *Materials* 2022; 15: 1152.
29. Vrabel’ M., Mankova I., Beno J., et al. Surface Roughness Prediction using Artificial Neural Networks when Drilling Udimet 720. *Procedia Eng* 2012; 48: 693–700.